

Structure of hydrated clusters of dibenzo- 18-crown-6-ether in a supersonic jet -Encapsulation of water molecules in the crown cavity-

*Ryoji Kusaka, Yoshiya Inokuchi, and Takayuki Ebata**

Department Chemistry, Graduate school of Science, Hiroshima University, Higashi-Hiroshima 739-
8526, Japan

Abstract

The structure of dibenzo-18-crown-6-ether (DB18C6) and its hydrated clusters has been investigated in a supersonic jet. Two conformers of bare DB18C6 and six hydrated clusters (DB18C6-(H₂O)_n) were identified by laser induced fluorescence, fluorescence detected UV-UV hole-burning and IR-UV double-resonance spectroscopy. The IR-UV double resonance spectra were compared with the IR spectra obtained by quantum chemical calculations at the B3LYP/6-31+G* level. The two conformers of bare DB18C6 are assigned to "boat" and "chair I" forms, respectively, among which the boat form is dominant. All the six DB18C6-(H₂O)_n clusters with $n = 1-4$ have a boat conformation in the DB18C6 part. The water molecules form a variety of hydration networks in the boat-DB18C6 cavity. In DB18C6-(H₂O)₁, a water molecule forms the bidentate

hydrogen bond with the O atoms adjacent to the benzene rings. In this cluster, the water molecule is preferentially hydrogen bonded from the bottom of boat-DB18C6. In the larger clusters, the hydration networks are developed on the basis of the DB18C6-(H₂O)₁ cluster.

Introduction

Crown ether is one of the well known host molecules, along with calixarene and cyclodextrin. These host molecules exhibit selective and cooperative encapsulation of ionic or neutral species, and play vital roles in various kinds of chemical application such as phase transfer catalyst¹ and separation of chiral species.² As can be seen in previous studies, the encapsulation is fairly controlled by the conformation of host molecules and the non-covalent interaction between host and guest molecules.³ Spectroscopic studies for host-guest complexes have been carried out mostly at room temperature by absorption, fluorescence, NMR, IR, and Raman spectroscopy.^{4,8} Since the energy scale of the non-covalent interaction in the complexes are comparable to the thermal energy, only averaged aspects of the host-guest complexes were examined in these studies. Matsuura et al. measured Raman spectra of 18-crown-6/water system at liquid nitrogen temperature.⁸ Ault et al. measured IR spectra of (18-crown-6)-ClF, -Cl₂, -HF, and -HCl complexes in argon matrix.^{9,10} In both cases, Raman and IR spectra become sharper and simpler than those at room temperature, suggesting that the cooling will be effective for shedding light on the details of the intermolecular interaction in the host-guest complexes, free from congested spectral features. Supersonic jet expansion is another powerful method for the cooling as well as for the solvent-free condition. Very recently, we first reported a laser spectroscopic study on jet-cooled benzo-18-crown-6-ether (B18C6) and dibenzo-18-crown-6-ether (DB18C6, scheme 1).¹¹ In the paper, we discussed the conformation of B18C6 and DB18C6, and the hydration structure of B18C6-(H₂O)₁ and DB18C6-(H₂O)₁.

In the present work, we report the structure of DB18C6-(H₂O)_n with $n = 0-4$, by using laser induced fluorescence (LIF), fluorescence-detected UV-UV hole-burning (HB), and IR-UV double-

resonance spectroscopy. We perform quantum chemical calculations to obtain probable structures and IR spectra of DB18C6-(H₂O)_n. From the spectroscopic and calculated results, we discuss the conformation of DB18C6 and the encapsulation structure of DB18C6-(H₂O)_n ($n = 1-4$).

Experimental

Details of the experiment were described in our previous papers.^{12,13} In brief, we used a home-made pulsed nozzle to generate jet-cooled DB18C6. We attached a sample housing made of poly-imido resin at the head of a commercially available nozzle (General Valve series 9). DB18C6 powder (Tokyo Kasei Kogyo) in the housing was heated to ~ 400 K. The mixture of DB18C6 and water vapor with helium carrier gas (with a total pressure of 2 bar) was injected into vacuum through the nozzle for generating a supersonic jet of DB18C6-(H₂O)_n. Partial pressure of water vapor was controlled by regulating the temperature of a water container which was connected to the gas line.

For the LIF spectroscopic measurements, an output of a pulsed UV laser (Inrad, Autotracker III (KDP) / Lambda Physik, Scanmate / Continuum, Surelite II) was introduced to the vacuum chamber at ~ 30 mm downstream from the nozzle. Fluorescence was collected by a series of lenses and detected by a photomultiplier tube (Hamamatsu Photonics, 1P28). For removing stray light, a glass filter (CVI, CG-WG-295) was placed before the photomultiplier tube. LIF spectra were obtained by plotting the fluorescence intensity as a function of UV frequency. For HB spectroscopy, the UV laser in the LIF measurement was used for a probe light. The frequency of the probe UV laser was fixed to a vibronic band of a single species and the fluorescence signal was monitored. A pump UV laser (Inrad, Autotacker II (KDP)/ Continuum, ND6000/ Continuum, Surelite II) was introduced to the jet at ~ 10 mm upstream of the probe position. The time interval between the pump and the probe light was fixed to $\sim 4 \mu\text{s}$. When the pump laser frequency is resonant to a transition of the species monitored, the species is excited to the upper state. This excitation by the pump laser causes depletion of the fluorescence signal by the probe light. Thus, the electronic spectrum of the monitored species was obtained as fluorescence dip spectra as a function of the

pump UV frequency. The experimental scheme of IR-UV double-resonance spectroscopy is similar to that of HB spectroscopy. An output of a tunable IR laser (Laser Vision/ Quanta-Ray, GCR250) was introduced coaxially with the UV probe laser ~ 100 ns prior to the probe pulse. The frequency of the IR pump laser was scanned while monitoring the fluorescence signal. Depletion of the fluorescence occurs when the IR frequency is resonant to a vibrational transition of the species monitored. IR spectra in the S_0 state were obtained as fluorescence dip spectra.

Geometry optimization and vibrational analysis were done at the B3LYP/6-31+G* level with GAUSSIAN 03 program package.¹⁴ A scaling factor of 0.9744 was employed to vibrational frequencies calculated for comparison with the IR-UV double-resonance spectra.

Results

1. LIF and HB spectra

Fig. 1(a) shows the LIF spectrum of jet-cooled DB18C6 in the origin band region. The spectrum was obtained under the condition with high water vapor pressure. The HB spectra measured by monitoring bands **m1**, **m2**, **a**, and **c–f** are shown in Figs. 1(b)–1(h). Since the HB spectra in Fig. 1 show different spectral features from each other, bands **m1**, **m2**, **a**, and **c–e** in the LIF spectrum are assigned to the origin bands of different species. The frequencies of the origin bands are listed in Table 1. Bands **m1** and **m2** are assigned to different conformers of bare DB18C6, because they do not exhibit any bands assignable to the OH stretching vibration in the IR spectra.¹¹ Bands **a–f** can be ascribed to hydrated clusters DB18C6-(H₂O)_{*n*}. These bands are very weak without the addition of water vapor. But their intensities increase drastically by adding water vapor to the sample gas, and the IR-UV double-resonance spectra for these bands show the OH stretching vibrations of water molecules, as shown later. In the HB spectra of **m2**, **a**, and **c–e**, the origin bands are accompanied by a band with a small interval of ~ 5 cm⁻¹, while the origin band of **m1** is isolated from other bands. Similar with the origin band, the HB spectra for **m2**, **a**, and **c–e** show several pairs of two bands which are separated by ~ 5 cm⁻¹.

2. IR-UV double-resonance spectra

Figs. 2(a)–2(f) show the IR-UV double-resonance spectra observed by probing bands **a–f** in the LIF spectrum. All the bands in this IR region are ascribed to the OH stretching vibration of water molecule(s). The IR spectra of **a** and **b** clearly show two OH stretching bands, suggesting that bands **a** and **b** in the LIF spectrum are due to DB18C6-(H₂O)₁. As seen in Fig. 2(c), the IR spectrum of band **c** displays four bands in this region. Therefore, band **c** is assignable to a DB18C6-(H₂O)₂ cluster. The IR spectra of **d–f** have more than four OH bands; bands **d–f** are attributed to DB18C6-(H₂O)_n with $n \geq 3$. Stick diagrams in the lower panels in Fig. 2 show the IR spectra calculated for optimized structures of DB18C6-(H₂O)_n with $n = 1–4$. Details of the calculated spectra, the optimized structures, and the assignment of the IR-UV double-resonance spectra are mentioned in the next section.

Discussion

1. Bare DB18C6: bands **m1** and **m2**

We first discuss the conformation of bare DB18C6 corresponding to bands **m1** and **m2**. We carried out geometry optimization of bare DB18C6 by DFT calculation at the B3LYP/6-31+G* level and obtained three conformers. Figs. 3(a)–3(c) show the stable conformers of bare DB18C6 and their total energies relative to that of the most stable one, which are given after the zero point energy correction. The most stable isomer is a "boat" form, which belongs to C_{2v} point group (Fig. 3(a)). The other two conformers are different types of "chair" forms (Figs. 3(b) and 3(c)), both of which belong to C_i point group. We call them "chair I" and "chair II". In our previous paper,¹¹ chair II was predicted to be the second most stable conformer. However, as seen in Fig. 3, we found another isomer (chair I) which is more stable than chair II. A major difference between the two chair forms is the conformation of four –O–CH₂– frames connecting to the benzene rings. In chair I, all the atoms of the –C–O–C=C–O–C– frame, where the C=C part of the frame stands for the carbon atoms of the benzene rings, is in the same plane. In chair II, two of the four –O–CH₂– frames are

twisted out of the planes. In Table 2, we list the observed transition energies and the $S_1 \leftarrow S_0$ and $S_2 \leftarrow S_0$ transition energies of the three conformers obtained by time dependent (TD)-DFT calculation at the B3LYP/6-31+G* level. The calculations show that the $S_1 \leftarrow S_0$ energy of chair I is the lowest among those of the three forms, while chair II shows the highest energy. The result that the transition energy of chair II is highest in the three conformers can be explained by the difference of the delocalization of the π -orbitals. The electronic transition of DB18C6 is essentially the π - π^* transition of dimethoxybenzene (DMB). The π - π^* transition energy decreases when the π -orbitals largely extend to the adjacent O atoms. This delocalization can occur for boat and chair I conformers, because all the atoms of the $-C-O-C=C-O-C-$ frames are in the same planes of the benzene rings. In chair II, on the contrary, the frames are twisted out of the benzene planes, resulting in less delocalization of the π -orbitals and higher $S_1 \leftarrow S_0$ energy than "boat" and "chair I" conformers. Thus, on the basis of relative energies and transition energies of the three conformers, band **m2**, which is much stronger than **m1** and located on the blue side of **m1** in the LIF spectrum, can be assigned to the boat conformer and **m1** is to chair I conformer. These assignments are reasonable since both boat and chair I conformers were found in a crystal.¹⁵

One noticeable feature of band **m2** is that this band is accompanied by low frequency bands with interval of 5 and 13 cm^{-1} , while band **m1** is isolated from other peaks. A possible assignment of such low frequency bands is the "butterfly" mode shown in scheme 2. By the DFT calculation in S_0 , we obtained the vibrational frequency of 21 cm^{-1} for the "butterfly" mode, which is the lowest frequency vibration in boat-DB18C6. Although the calculated frequency is for S_0 , the 5 cm^{-1} interval seems too low and the 13 cm^{-1} band is more probable to be assigned to the "butterfly" mode in S_1 . Interestingly, in the HB spectrum of Fig. 2(c) the 13 cm^{-1} band is also accompanied by another band with a 5 cm^{-1} interval. Therefore, it is quite probable that the bands accompanied with the 5 cm^{-1} interval is not due to the lowest frequency vibronic band.

The possible assignment of the 5 cm^{-1} band is due to exciton splitting. DB18C6 is regarded as a combination of two DMB moieties. The excited states of DB18C6 can be expressed by linear

combinations of $\phi_A^* \cdot \phi_B$ and $\phi_A \cdot \phi_B^*$:

$$S_1: \quad \phi_A^* \cdot \phi_B + \phi_A \cdot \phi_B^* \quad (1a)$$

$$S_2: \quad \phi_A^* \cdot \phi_B - \phi_A \cdot \phi_B^* \quad (1b)$$

where ϕ^* and ϕ stand for wavefunctions of DMB in the S_1 and S_0 states, respectively. For the boat form, which has C_{2v} symmetry, transitions from the $S_0(A_1)$ state to both the $S_1(B_1)$ and the $S_2(A_1)$ states are dipole allowed. On the contrary, in the chair forms, which have C_i symmetry, only the transition to the $S_1(A_u)$ state is dipole allowed. Therefore, the 5 cm^{-1} splitting of m2 can correspond to the S_2 - S_1 energy difference of boat-DB18C6, while the splitting does not appear in chair-DB18C6 due to symmetrical reason. In the weak interaction model, the S_2 - S_1 spitting energy of a molecule having equivalent two chromophores is given by ^{16,17}

$$\Delta E = 2FV_{AB} \quad (2)$$

, where

$$V_{AB} = \frac{\mu_A \cdot \mu_B}{4\pi\epsilon_0 R_{AB}^3} (2\cos\theta_A \cos\theta_B - \sin\theta_A \sin\theta_B \cos\varphi) \quad (3)$$

R_{AB} is the distance between the two centers of the chromophores, θ_A and θ_B are the angles of the transition dipole moment to the line connecting the two centers, and φ is the dihedral angle between the two transition dipoles (scheme 3). V_{AB} is the electronic part and F , which is the Franck-Condon factor on the transition, is the vibrational part. To obtain V_{AB} , we first calculated the oscillator strength for the $S_1 \leftarrow S_0$ transition of DMB at the TD-DFT B3LYP/6-31+G* level. The calculated $S_1 \leftarrow S_0$ oscillator strength of DMB is 0.049, which corresponds to the transition dipole moment of $\mu_{S_1 \leftarrow S_0} = 5.5 \times 10^{-30} \text{ C}\cdot\text{m}$. In boat-DB18C6, the values of θ_A , θ_B , φ and R_{AB} are 320° , 220° , 0° , and 8.8 \AA , respectively. By using these values, we obtain 70 cm^{-1} for $2V_{AB}$. The validity of the estimation of the 70 cm^{-1} S_2 - S_1 exciton splitting energy in boat-DB18C6 is supported by the TD-DFT calculation given in Table 2; from the $S_1 \leftarrow S_0$ and $S_2 \leftarrow S_0$ transition energies, we obtain 82 cm^{-1}

for the S_2 - S_1 energy difference of boat-DB18C6. Estimation of the vibrational part F in eq. (2) is difficult, because we do not know the Franck-Condon factor of the $S_1 \leftarrow S_0$ transition. Instead, we estimated F from the relative transition intensity of the origin band from the LIF and UV-UV hole burning spectra in Fig. 2(a) and 2(c). A roughly estimated ratio of the origin band LIF intensity to the total LIF intensity is $\sim 10\%$. This value and the calculated ΔE give 7 cm^{-1} for the origin band splitting. Though this estimated value may have a large uncertainty, the value is in reasonable agreement with the experimental observation (5 cm^{-1}). Therefore, the 5 cm^{-1} split of band **m2** can be described to the exciton splitting.

2. DB18C6-(H₂O)₁: Bands **a** and **b**

The HB spectrum of band **a** (Fig. 1(d)) shows a doublet structure with 5 cm^{-1} interval, similar to the HB spectrum of **m2**, indicating that the DB18C6 component of the species of band **a** has a boat form. Fig. 2(a) shows the IR-UV spectrum of band **a** in the OH stretching region. The spectrum of band **a** has already been reported in our previous paper.¹⁰ Since two bands appear in the spectrum, band **a** is assigned to DB18C6-(H₂O)₁. The intensities of the two bands are comparable with each other. In addition, their band positions (3580 and 3648 cm^{-1}) are lower than the symmetric and anti-symmetric stretching OH vibrations of a water molecule by 77 and 108 cm^{-1} . Thus, the two OH groups of the water molecule take part in the hydrogen bond (H-bond) as a double hydrogen donor (bidentate). In the LIF spectrum, band **a** is located at 89 cm^{-1} higher frequency from band **m2**. The magnitude of the blue-shift is similar to that of DMB-(H₂O)₁ with respect to bare DMB (127 cm^{-1}).¹⁹ In DMB-(H₂O)₁, a water molecule is bound to the O atoms of the methoxy groups via two O-H \cdots O hydrogen-bonds. Thus, the similarity of the blue-shift indicates that in the species of band **a** the OH groups of the water molecule are bonded to the O atoms next to the benzene rings. The IR-UV double-resonance spectrum of band **b** (Fig. 2(b)) shows two OH stretching bands with positions different from those of band **a** (Fig. 2(a)). Therefore, band **b** is assigned to another DB18C6-(H₂O)₁ isomer with a bidentate H-bond. The frequencies of the two OH stretching vibrations are slightly higher for **b**, suggesting weaker bidentate H-bond in the band **b**

species. Band **b** is not so largely apart from band **a** in the LIF spectrum. Therefore, the band **b** species may probably have a boat conformer like the band **a** species.

For DB18C6-(H₂O)_n, it is quite time-consuming work to find all the structures by quantum chemical calculations. Thus, in this work, we try to search particular isomers which reproduce the observed IR spectra. Fig. 4(a) and 4(b) show two optimized structures of DB18C6-(H₂O)₁ with boat conformation (W1-I and W1-II). In these structures, a water molecule is H-bonded to the O atoms adjacent to the benzene rings of DB18C6 as a bidentate form. In W1-I, the OH groups of the water molecule point to the middle positions between O₁ and O₄ and between O₁₀ and O₁₃, and the cluster has C_{2v} symmetry. In W1-II, the OH groups are bonded directly to O₄ and O₁₀. The IR spectra calculated for W1-I and W1-II are shown in the lower panels of Fig. 2(a) and 2(b) as stick diagram. Both W1-I and W1-II display the symmetric and anti-symmetric OH stretching vibrations around ~3600 and ~3700 cm⁻¹, respectively. These IR spectra well coincide with the IR-UV spectra of bands **a** and **b**. We attribute bands **a** and **b** to W1-I and W1-II, respectively, because the OH stretching frequencies of W1-I are slightly lower than those of W1-II, which reproduce the IR-UV spectra of bands **a** and **b**. The effect of the bidentate H-bond like W1-I is seen in the HB spectrum of band **a**. As described above, we assigned the vibronic band at 13 cm⁻¹ above band **m2** to the butterfly vibration. The HB spectrum of band **a** shows that the frequency of this vibration increases to 20 cm⁻¹. This increase indicates that the bidentate water molecule in W1-I makes the crown-ether frame more rigid and the frequency of the butterfly vibration higher than bare DB18C6.

The stronger H-bond in W1-I than W1-II can be examined with the charge distribution. Fig. 5(a) and 5(b) show a top and bottom view of the electrostatic potential of boat-DB18C6. The negative charge on O₁, O₄, O₁₀, and O₁₃ atoms is well exposed to the bottom. Therefore, a water molecule can form the H-bond to O₁, O₄, O₁₀, and O₁₃ atoms more strongly on the bottom side (W1-I) than on the top side (W1-II). Fig. 5(c) and 5(d) show a top and bottom view of the electrostatic potential of W1-I. Formation of the H-bond with a water molecule makes the negative charge on O₁, O₄, O₁₀, and O₁₃ atoms relatively smaller than the case of bare DB18C6. On the other hand, the O

atom of the water molecule has large negative charge; the Mulliken charge of the water O atom is –1.1. This charge in W1-I plays a very important role for the H-bond formation with additional water molecules.

3. DB18C6-(H₂O)₂: band c

The HB spectrum of band c (Fig. 1(e)) also exhibits a doublet structure of ~5 cm⁻¹ interval. Thus, the DB18C6 component in the band c species also has boat form. The IR-UV double-resonance spectrum of band c (Fig. 2c) shows four OH stretching bands, indicating that band c is attributed to DB18C6-(H₂O)₂. By the comparison of the IR spectra of bands a and c, we can assign the IR bands at 3562 and 3623 cm⁻¹ in Fig. 2(c) to the symmetric and anti-symmetric OH stretching vibrations of a bidentate water, which are red-shifted by 18 and 25 cm⁻¹ from those of band a (Fig. 2(a)), respectively. The red-shift of the two OH stretching vibrations of the bidentate water implies that the O atom of the bidentate water accepts the second water molecule. The bands at 3401 and 3716 cm⁻¹ can be assigned to the H-bonded and free OH stretching vibrations of the second water molecule, respectively. The H-bonded OH stretching frequency (3401 cm⁻¹) is quite lower than that of water molecule with the normal σ -type H-bond. For example, the frequency of the H-bonded OH stretching vibration in water dimer, (H₂O)₂, is 3530 cm⁻¹.¹⁹ Therefore, the H-bond of the second water molecule in the band c species is much stronger than that in (H₂O)₂.

Fig. 4(c) shows the most probable structure for the species of band c (W2-I). In W2-I, the second water molecule (w₂) is H-bonded to the O atom of the bidentate water molecule (w₁). The IR spectrum calculated for W2-I is shown in Fig. 2(c). The red-shift of the symmetric and anti-symmetric vibrations of w₁ in W2-I is 17 and 25 cm⁻¹ from those of W1-I, respectively. These values are similar to the red-shifts of the OH stretch bands of band a with respect to those of band c (18 and 25 cm⁻¹). As shown in Fig. 5(d), the O atom of the bidentate water molecule is strongly negatively charged in W1-I, which is a good target of the H-bond. Thus, the second water molecule (w₂) is strongly H-bonded to the first water (w₁).

4. DB18C6-(H₂O)₃: band **d**

On the basis of the doublet feature for band **d** (Fig. 1(f)), we can say that the DB18C6 component in the band **d** species also has a boat form. Fig. 2(d) shows the IR-UV spectrum of band **d**. There are six OH stretching bands in the spectrum; band **d** in the LIF spectrum can be assigned to DB18C6-(H₂O)₃. Different from the IR spectrum of band **c**, all the bands are located close to each other and no band is observed at the position of the free OH band ($\sim 3715\text{ cm}^{-1}$). This result suggests that in this cluster there is no single-donor water molecule and all the water molecules form the bidentate H-bond. On the basis of the IR band positions in Fig. 2(a) and 2(b), we classify the six bands in Fig. 2(d) into three pairs: (1) 3575 and 3648 cm^{-1} , (2) 3601 and 3663 cm^{-1} , and (3) 3627 and 3685 cm^{-1} . The lower and higher frequency bands for each pair are assignable to the symmetric and anti-symmetric OH stretching vibrations, respectively. The frequencies of the lowest frequency pair (3575 and 3648 cm^{-1}) are very close to those of band **a** (3580 and 3648 cm^{-1}). Therefore, this pair can be assigned to a bidentate water molecule bonded on the bottom of the boat conformer like W1-I. The frequencies of the other two pairs are close to those of band **b** (3606 and 3679 cm^{-1}). Thus, the water molecules corresponding to these pairs are thought to form weaker bidentate H-bonds on the top of the boat form like W1-II.

From the IR spectral feature, the band **d** species has one and two water molecule(s) on the bottom and the top sides of a boat conformer, respectively. Fig. 4(d) (W3-I) represents the most probable structure of band **d**. This cluster belongs to C_{2v} point group. In this structure, one molecule (w_1) is on the bottom side of boat-DB18C6 and forms the bidentate H-bond like W1-I. The other two water molecules (w_2 and w_3) are located on the top side and form two bidentate H-bonds to the O atoms near the benzene rings like W1-II. The IR spectrum calculated for W3-I is shown in Fig. 2(d). Although each of the bands at ~ 3650 and $\sim 3730\text{cm}^{-1}$ seems to be a single band, there are two close bands assignable to w_2 and w_3 at each position. The positions of the six bands of W3-I agree with those of the IR-UV spectrum of band **d**.

5. DB18C6-(H₂O)₄: bands **e** and **f**

The doublet feature in the HB spectrum of band **e** (Fig. 1(g)) also suggests a boat conformer in the band **e** species. Fig. 2(e) shows the IR-UV spectrum measured by monitoring band **e**. Seven bands are clearly observed, and the band at 3620 cm⁻¹ has a shoulder on the higher frequency side. Therefore, band **e** in the LIF spectrum is assigned to DB18C6-(H₂O)₄. The 3422 and 3716 cm⁻¹ bands are assigned to the H-bonded and free OH stretching vibrations of a single-donor water, respectively. The band positions are similar to the lowest and the highest bands of **c** (Fig. 2(c), 3401 and 3716 cm⁻¹). Therefore, in the band **e** cluster, there is a single-donor water molecule like *w*₂ in W2-I. This result also implies that there is a water molecule corresponding to *w*₁ in W2-I. From the band positions of *w*₁ in Fig. 2(c) (3562 and 3623 cm⁻¹), the 3553 and 3620 cm⁻¹ bands in Fig. 2(e) can be ascribed to the *w*₁ molecule in the band **e** species. The bands at 3596, 3643, and 3686 cm⁻¹ along with the shoulder near the 3620 cm⁻¹ band in Fig. 2(e) are close to the 3601, 3627, 3663, and 3685 cm⁻¹ bands in Fig. 2(d), suggesting that there are also two bidentate water molecules like *w*₂ and *w*₃ of W3-I in the band **e** species. Unfortunately, in our quantum chemical calculations we cannot obtain any optimized DB18C6-(H₂O)₄ isomer whose IR spectrum matches the observed IR spectrum. Instead, we present a probable structure (W4-I) of band **e** in Fig. 4(e). In this structure, *w*₁, *w*₃, and *w*₄ are H-bonded similar to W3-I, and *w*₂ is H-bonded to *w*₁ similar to W2-I.

Fig. 2(f) shows the IR-UV double-resonance spectrum of band **f**. From the similarity of the IR band position, the 3438 cm⁻¹ band can be assigned to the single-donor OH vibration of a water molecule like *w*₂ in W2-I. The band at 3714 cm⁻¹ is assigned to the free OH stretching vibration of the same water molecule. Since only one peak is observed in the free OH stretching region, there is one single-donor water molecule in the band **f** species. The 3529 cm⁻¹ band is characteristic of the IR spectrum of band **f**; the other observed IR spectra in Fig. 2 do not show a band around 3529 cm⁻¹. The 3529 cm⁻¹ band is located on the lower frequency side of the bands of the bidentate water molecules like *w*₁–*w*₃ of W3-I. In addition, the width of the 3529 cm⁻¹ band is much broader than those of the bidentate water molecules. Therefore, the 3529 cm⁻¹ band cannot be assigned to a

bidentate water molecule to the ether ring. It is necessary to consider a different type of H-bond for the 3529 cm^{-1} band.

In Fig. 4(f) (W4-II) is shown a probable structure for band **f**. In W4-II, w_1 and w_2 construct the bidentate and single-donor H-bonded network like W2-I. The water molecules labeled by w_3 and w_4 are located on the top side of boat-DB18C6 and form a new H-bond network. One water molecule (w_3) is bonded to the ether O atoms (O_4 and O_{10}) with a bidentate manner, and the other one (w_4) forms a bridge between an ether O atom (O_{16}) and the O atom of w_3 . This type of the H-bond network was also found in the 18-crown-6-ether/water system at liquid nitrogen temperature.⁸ The IR spectrum calculated for W4-II is displayed in Fig. 2(f). As connected by solid lines, the IR spectrum calculated for W4-II well reproduces the IR-UV spectrum observed for band **f**. In particular, the calculation predicts a band at $\sim 3500 \text{ cm}^{-1}$, which is the stretching vibration of w_4 bonded to the O atom of w_3 . This band corresponds to the band at 3529 cm^{-1} in the IR-UV spectrum observed for band **f**.

Summary

The electronic and IR spectra of jet-cooled DB18C6-(H₂O)_{*n*} (*n* = 0–4) have been observed by LIF, UV-UV hole-burning, and IR-UV double-resonance spectroscopy. With the aid of quantum chemical calculations (B3LYP/6-31+G*), we have revealed detailed pictures of hydrated DB18C6 structures. For bare DB18C6, two conformers were identified as "boat" form and "chair-I" form, in which the boat conformer is dominant. All the electronic transitions of six hydrated clusters appear in higher frequency region compared with bare DB18C6 and shift to blue with increasing the cluster size. The H-bond networks are mainly constructed on the boat conformer. In DB18C6-(H₂O)₁, two isomers have been identified (W1-I and W1-II). In these isomers, a water molecule forms a bidentate H-bond to the O atoms connected to the benzene rings from the bottom (W1-I) and from the top (W1-II) of boat-DB18C6. In DB18C6-(H₂O)_{*n*} with *n* \geq 2, the H-bond network grows on the basis of W1-I. On the bottom side of W1-I, a water molecule is further H-bonded to the O atom of

the bidentate water molecule. On the top side, two types of H-bond networks are formed by two water molecules: (1) both water molecules are independently H-bonded to the four ether O atoms (O₁, O₄, O₁₀, and O₁₃) adjacent to the benzene rings by the bidentate manner, (2) one water molecule has a bidentate H-bond with the O₄ and O₁₀ atoms, and the other water molecule forms a bridge between the O atom of the bidentate water molecule and the O₁₆ atom of the ether frame. Thus, the present work revealed that DB18C6 has a high ability of encapsulating of water molecules with a variety of H-bond network.

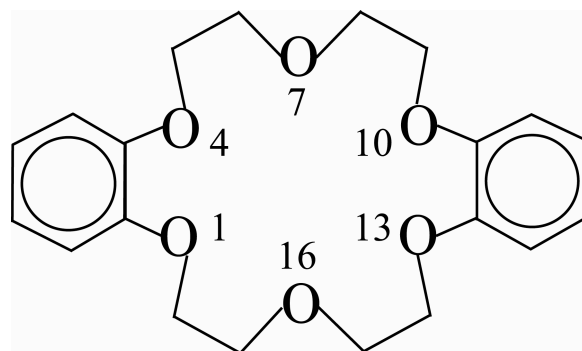
Acknowledgements

We gratefully thank Dr. Y. Yamada for valuable discussion from Kobe University. This work is supported by JSPS through a Grant in-Aid project (# 18205003 and # 19655004) and by the MEXT, Japan through the Grant-in-Aid for the Scientific Research on Priority Area "Molecular Science for Supra Functional Systems" [477].

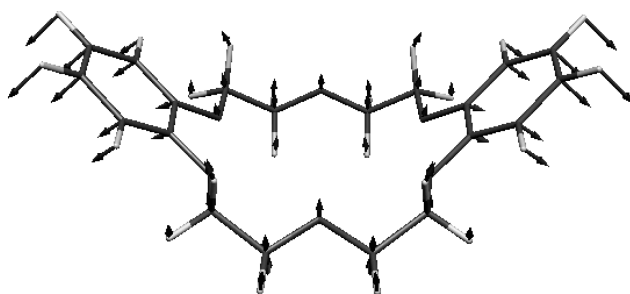
Reference

- 1 A. M. Stuart, J. A. Vidal, *J. Org. Chem.*, 2007, **72**, 3735.
- 2 M. H. Hyun, S. C. Han, H. J. Choi, B. S. Kang, H. J. Ha, *J. Chromatogr. A*, 2007, **1138**, 169.
- 3 A. Bogdanova, M. W. Perkovic, V. V. Popik, *J. Org. Chem.*, 2005, **70**, 9867.
- 4 Y. V. Fedorov, O. Fedorova, N. Schepel, M. Alfimov, A. M. Turek, J. Saltiel, *J. Phys. Chem. A*, 2005, **109**, 8653.
- 5 G. W. Buchanan, M. F. Rastegar, *Solid State Nucl. Magn. Reson.*, 2001, **20**, 137.
- 6 A. S. Denisova, E. M. Dem'yanchuk, G. L. Starova, L. A. Myund, A. A. Makarov, A. A. Simanova, *J. Mol. Structure*, 2007, **828**, 1.

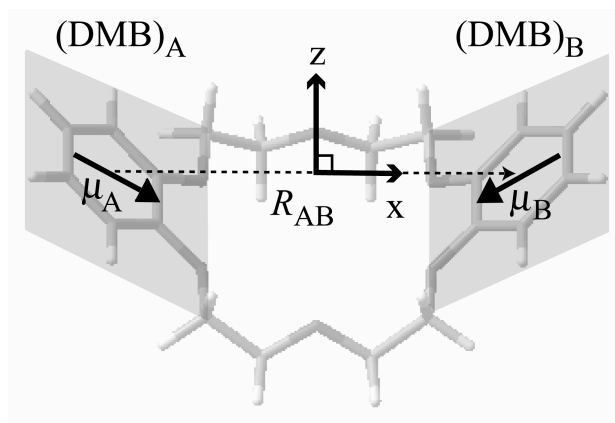
- 7 C. Endicott, H. L. Strauss, *J. Phys. Chem. A*, 2007, **111**, 1236.
- 8 K. Fukuhara, M. Tachikake, S. Matsumoto, H. Matsuura, *J. Phys. Chem.*, 1995, **99**, 8617.
- 9 H. Bai, B. S. Ault, *J. Mol. Struct.*, 1989, **196**, 47.
- 10 B. S. Ault, *J. Mol. Struct.*, 1989, **93**, 279.
- 11 R. Kusaka, Y. Inokuchi, T. Ebata, *Phys. Chem. Chem. Phys.*, 2007, **9**, 4452.
- 12 T. Ebata, T. Hashimoto, T. Ito, Y. Inokuchi, F. Altunsoy, B. Brutschy, P. Tarakeshwar, *Phys. Chem. Chem. Phys.*, 2006, **8**, 4783.
- 13 Y. Inokuchi, Y. Kobayashi, T. Ito, T. Ebata, *J. Phys. Chem. A*, 2007, **111**, 3209.
- 14 M. J. Frisch et al., Gaussian 03, Revision B.05, Gaussian, Inc., Pittsburgh PA, 2003.
- 15 D. Bright, M. R. Truter, *J. Chem. Soc. B*, 1970, **8**, 1544.
- 16 A. Müller, F. Talbot, S. Leutwyler, *J. Chem. Phys.*, 2002, **116**, 2836.
- 17 J. E. Wessel, J. A. Syage, *J. Phys. Chem.* 1990, **94**, 737.
- 18 J. T. Yi, J. W. Ribblett, D. W. Pratt, *J. Phys. Chem. A*, 2005, **109**, 9456.
- 19 Z. S. Hang, R. E. Miller, *J. Chem. Phys.*, 1989, **91**, 6613.



Scheme 1 DB18C6



Scheme 2



Scheme 3 Symmetry axes and transition dipole moments of boat-DB18C6

Table 1 Band positions of the origin for bare DB18C6 and its hydrated clusters

Position / cm^{-1}	Label	Assignment
35597	m1	DB18C6
35688	m2	DB18C6
35777	a	DB18C6-(H ₂ O) ₁
35800	b	DB18C6-(H ₂ O) ₁
35835	c	DB18C6-(H ₂ O) ₂
35858	f	DB18C6-(H ₂ O) ₄
35912	d	DB18C6-(H ₂ O) ₃
35955	e	DB18C6-(H ₂ O) ₄

Table 2 Transition energy (cm^{-1}) and oscillator strength of $S_1 \leftarrow S_0$ and $S_2 \leftarrow S_0$. The calculated values are obtained at the TD-B3LYP/6-31+G* level

		transition energy / cm^{-1}				oscillator strength	
		obs.		calc.		calc.	
		$S_1 \leftarrow S_0$	$S_2 \leftarrow S_0$	$S_1 \leftarrow S_0$	$S_2 \leftarrow S_0$	$S_1 \leftarrow S_0$	$S_2 \leftarrow S_0$
boat	(C_{2v})	35688	35693	39640	39722	0.0928	0.0347
chair I	(C_i)	35597		39608	39688	0.1382	0
chair II	(C_i)			40133	40145	0.0963	0

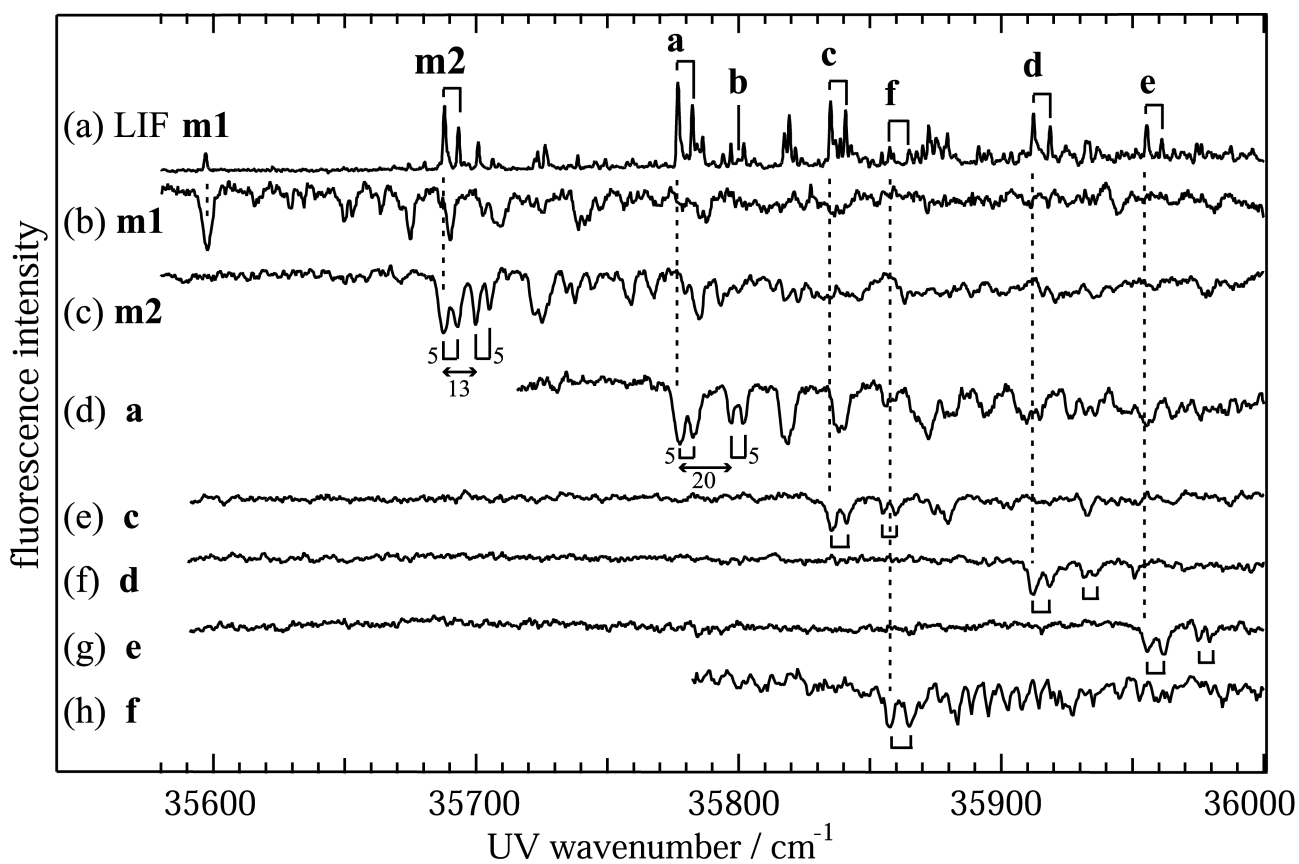


Fig. 1 (a) LIF spectrum of DB18C6. (b)-(h) UV-UV hole-burning spectra measured by monitoring bands **m1**, **m2**, **a**, and **c-d** in the LIF spectrum. The numbers in (c) and (d) show the interval (cm^{-1}) between the adjacent bands.

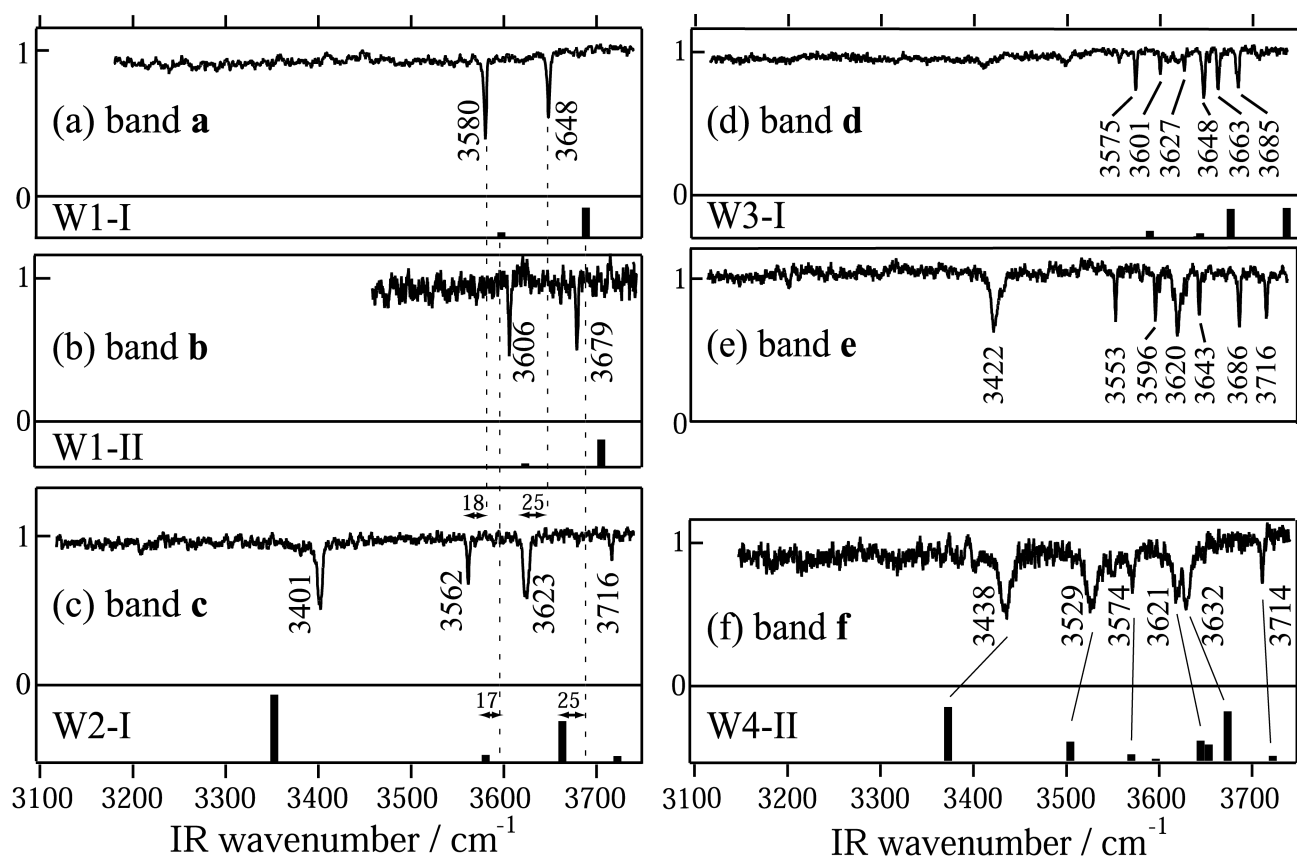


Fig. 2 IR-UV spectra measured by monitoring bands **a-f** in the LIF spectrum. Sticks in each of the panels show IR spectra calculated for optimized structures.

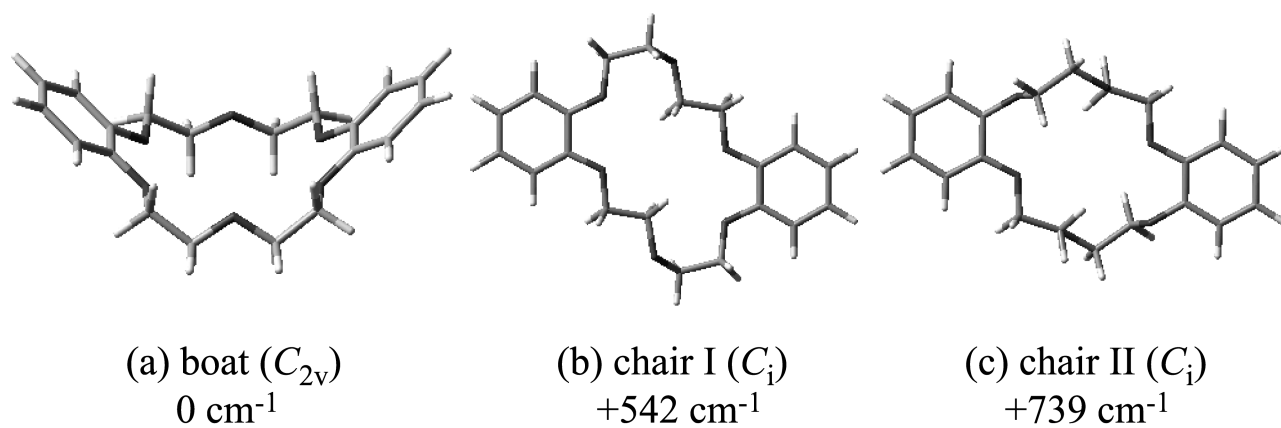


Fig. 3 Optimized conformers for bare DB18C6: (a) boat, (b) chair I, and (c) chair II. The numbers in the figure represent the total energies relative to that of the most stable conformer (boat). The total energies are corrected by the zero-point vibrational energy.

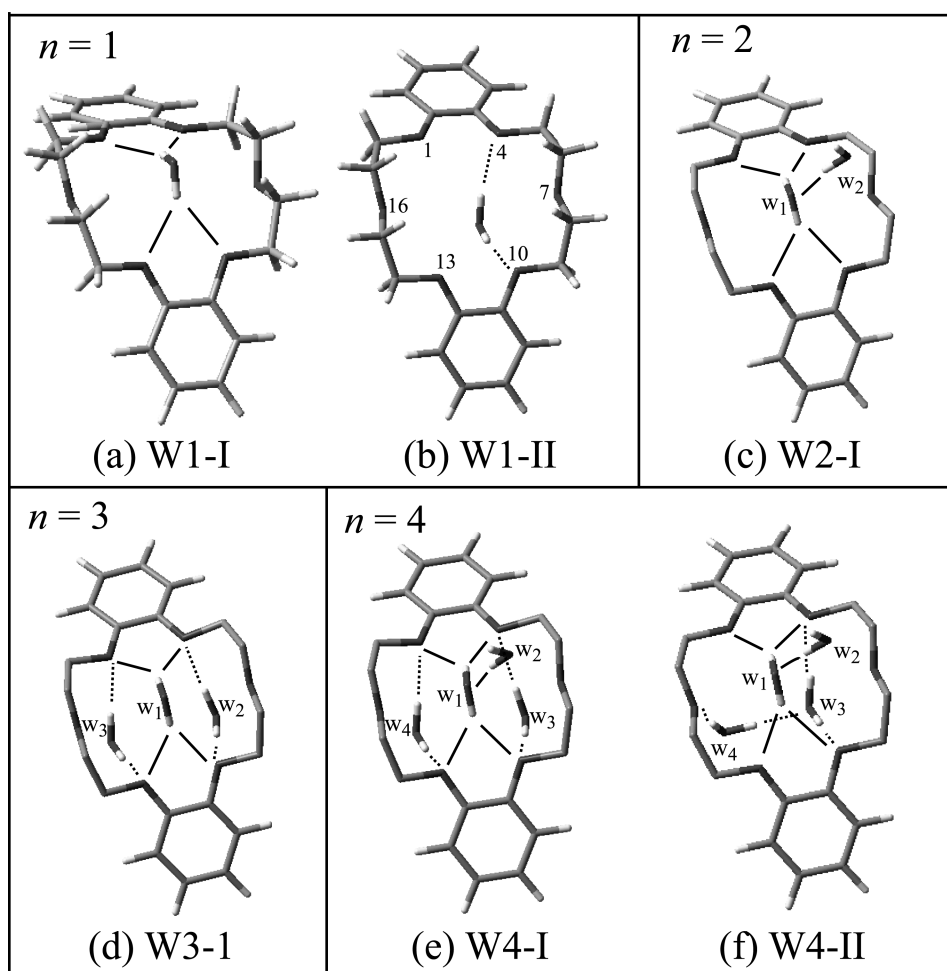


Fig. 4 Optimized structures of DB18C6-(H₂O)_n. Solid lines show H-bond on the bottom side of boat-DB18C6 and dotted lines on the top side. Alkyl hydrogen atoms are not shown for $n = 2-4$.

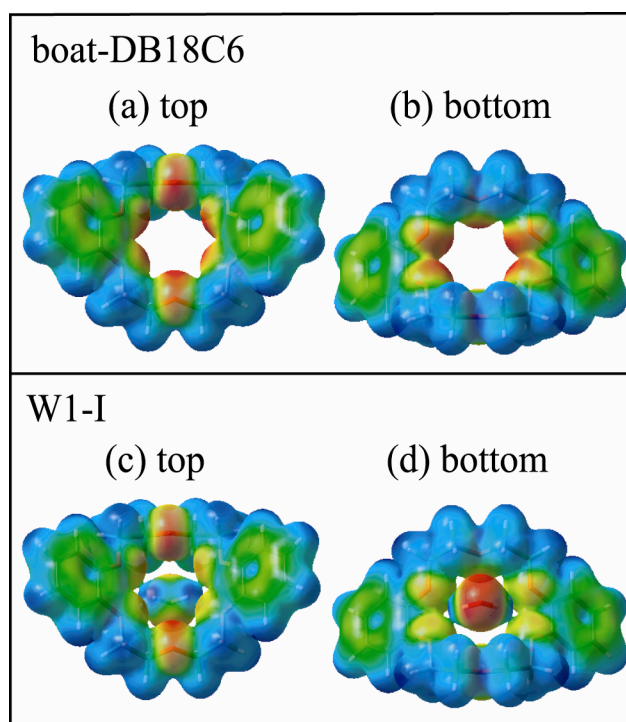
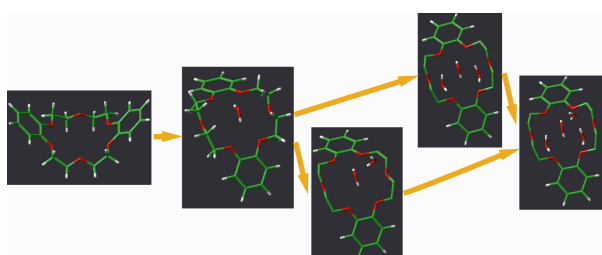


Fig. 5 Electrostatic potential from -0.08 a.u. (red) to $+0.08$ a.u. (blue) on the surface of the same electron density ($0.01 e/a_0^3$).

A graphical and textual abstract



The growth of hydrogen-bonding networks of water clusters inside the crown cavity has been studied for dibenzo-18-crown-6-ether in a supersonic beam.